Characterising galaxy clusters' completeness in Planck with hydrodynamical simulations

Stefano Gallo, Marian Douspis, Elie Soubrié, Laura Salvati

https://arxiv.org/abs/2309.11544

CMB-France, 05/12/2023

Galaxy Cluster detection with SZ effect

We can use CMB surveys (e.g. ***Planck* satellite**) to **detect** galaxy clusters

How? → **MMF**

Melin et al. (2006)

- **Characteristic spectral shape**
- **+**
- **Cluster profile template**

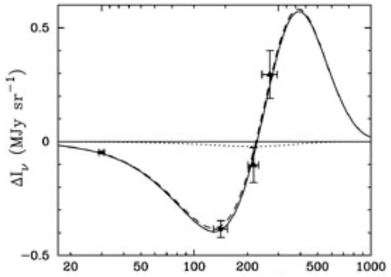

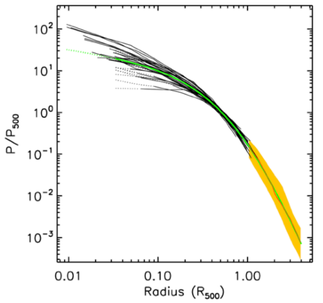

(Arnaud+2010)

→ Catalog of detections

But → several assumptions: **self-similarity**, **spherical symmetry**, … → Need for **precise characterisation of the cluster sample**

Cosmology with Galaxy Clusters

Galaxy clusters number counts → depend on cosmological parameters: Ω_m, σ_8, …

Different ingredients are needed to compare the observed counts with the theory:

$$\frac{\mathrm{d}N}{\mathrm{d}z} = \int \mathrm{d}\Omega \int \mathrm{d}M_{500}\, \hat{\chi}\left(z, M_{500}, l, b\right) \frac{\mathrm{d}N}{\mathrm{d}z\ \mathrm{d}M_{500}\ \mathrm{d}\Omega}$$

Halo mass function

$$\hat{\chi} = \int \mathrm{d}Y_{500} \int \mathrm{d}\theta_{500} P\left(z, M_{500} \mid Y_{500}, \theta_{500}\right) \chi\left(Y_{500}, \theta_{500}, l, b\right)$$

Scaling relations **Selection Function**

Selection Function

One of the main ingredients in cosmological analyses:

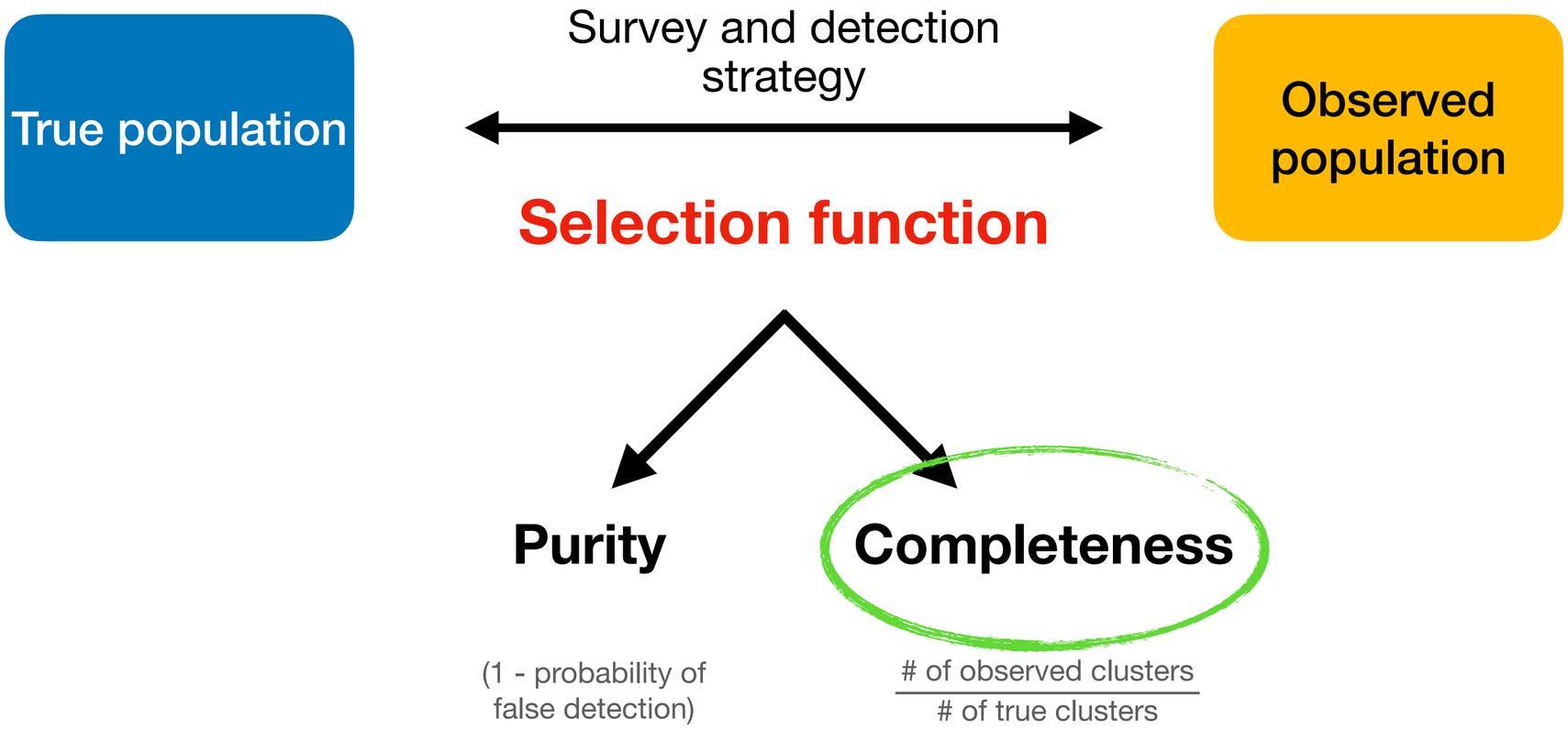

Selection Function

One of the main ingredients in cosmological analyses:

Purity

(1 - probability of false detection)

Completeness

$$\frac{\text{\# of observed clusters}}{\text{\# of true clusters}}$$

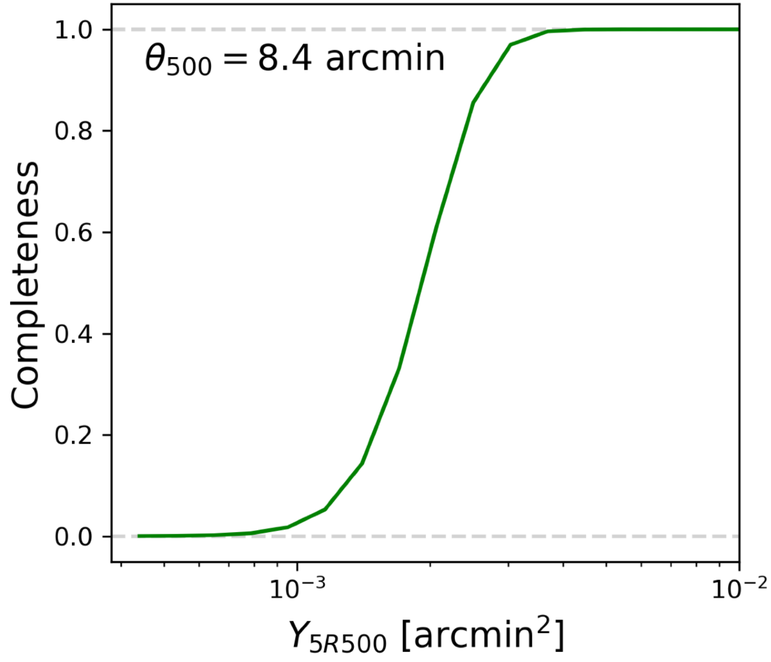

Selection Function

One of the main ingredients in cosmological analyses:

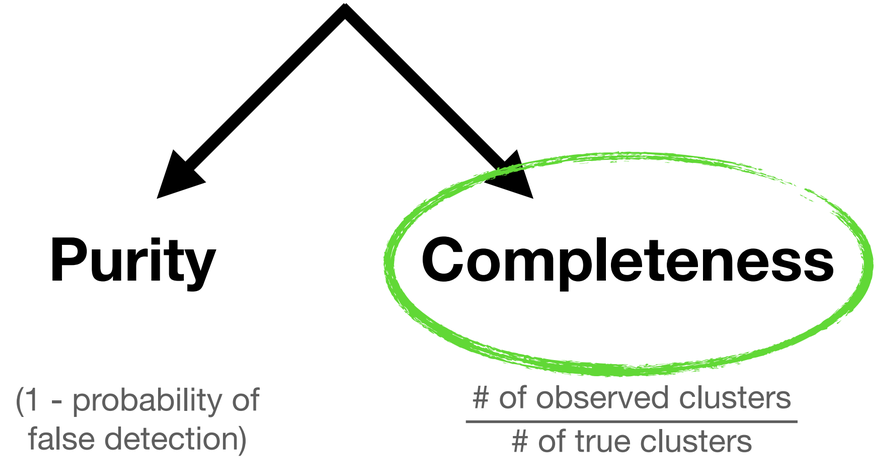

Incorrect characterisation

=

Possible biases in cosmological parameters

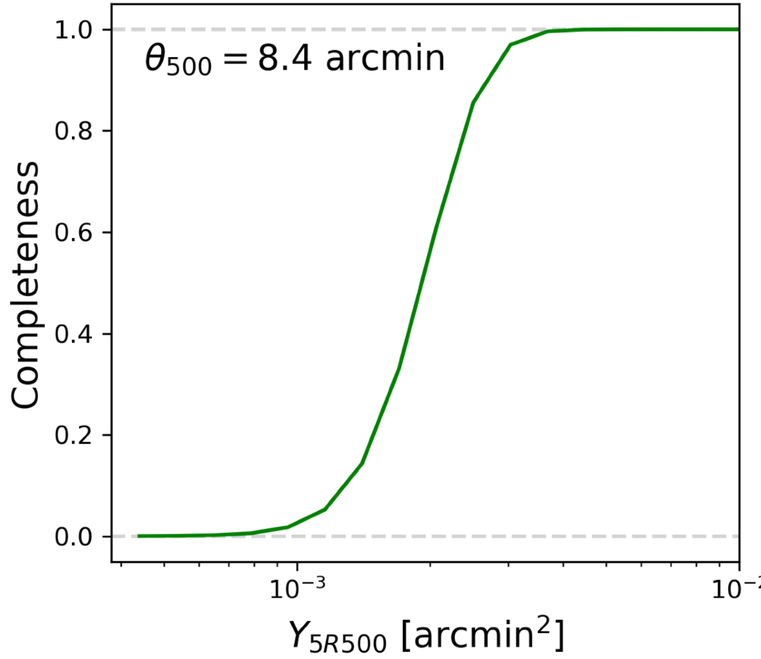

Completeness

- If one assumes **Gaussian errors** on the Compton-y signal, the completeness can be estimated as:

$$P\left(d \mid Y_{5R500}, \sigma\left(\theta_{500}\right), q\right) = \frac{1}{2}\left[1 + \mathrm{erf}\left(\frac{Y_{5R500} - q\,\sigma\left(\theta_{500}\right)}{\sqrt{2}\sigma\left(\theta_{500}\right)}\right)\right]$$

PlanckXX(2013), PlanckXXIV(2015)

- **Another approach**: **inject** simulated cluster signals in the Planck frequency maps, and check how many are **recovered** by the detection algorithm

Completeness

- If one assumes **Gaussian errors** on the Compton-y signal, the completeness can be estimated as:

$$P\left(d \mid Y_{5R500}, \sigma\left(\theta_{500}\right), q\right) = \frac{1}{2}\left[1 + \mathrm{erf}\left(\frac{Y_{5R500} - q\,\sigma\left(\theta_{500}\right)}{\sqrt{2}\sigma\left(\theta_{500}\right)}\right)\right]$$

PlanckXX(2013), PlanckXXIV(2015)

- **Another approach**: **inject** simulated cluster signals in the Planck frequency maps, and check how many are **recovered** by the detection algorithm

Spherical images

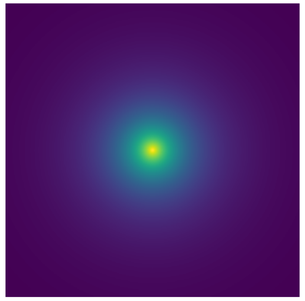

Simulation images

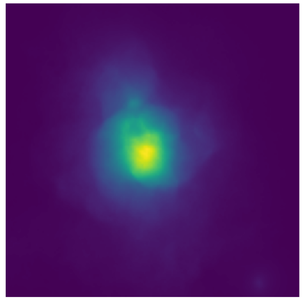

Injected Cluster Images

Simulation images

- IllustrisTNG-300 hydrodynamical simulation
- $M_{500} \gtrsim 1 - 2 \times 10^{14} M_{\odot}$
- $0.05 < z < 0.3$
- 6 projections per cluster
  ⟶ almost 9000 images

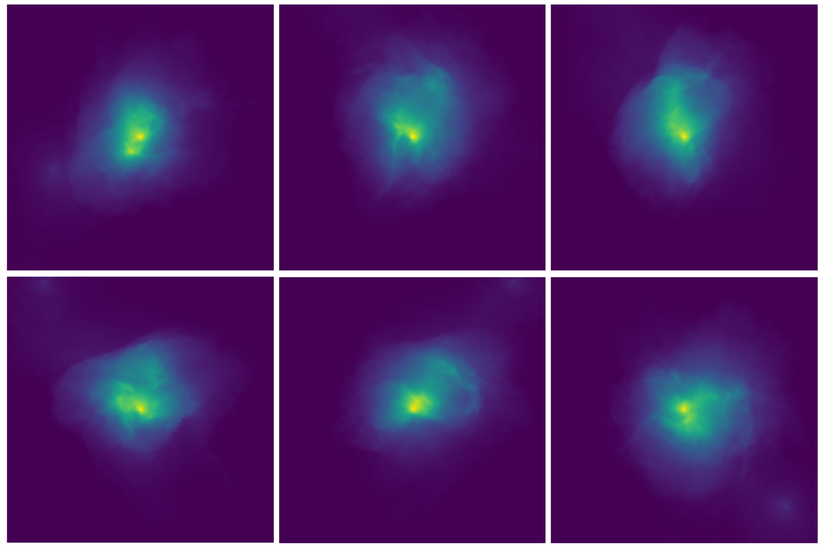

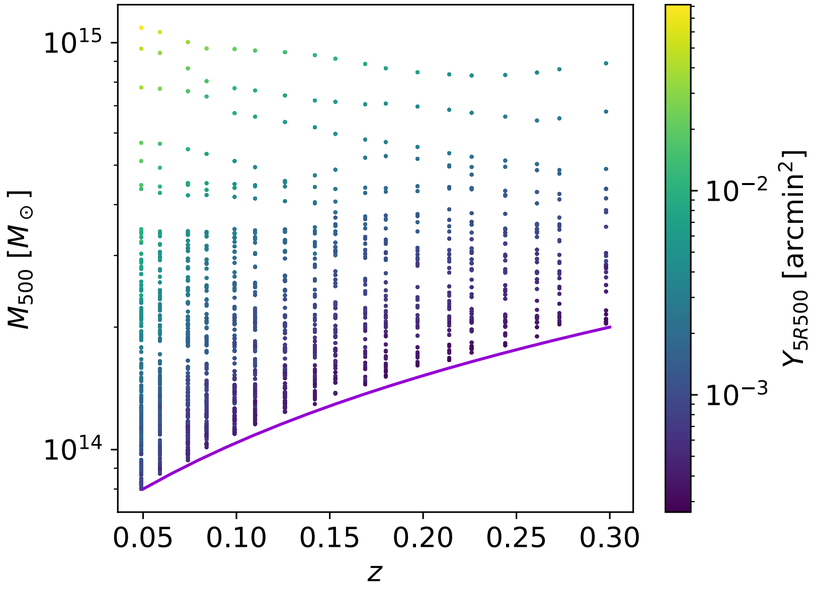

Spherical images

- Integrated gNFW profile (Arnaud+2010)
- Same $(Y_{5R500}, \theta_{500})$ distribution as simulation

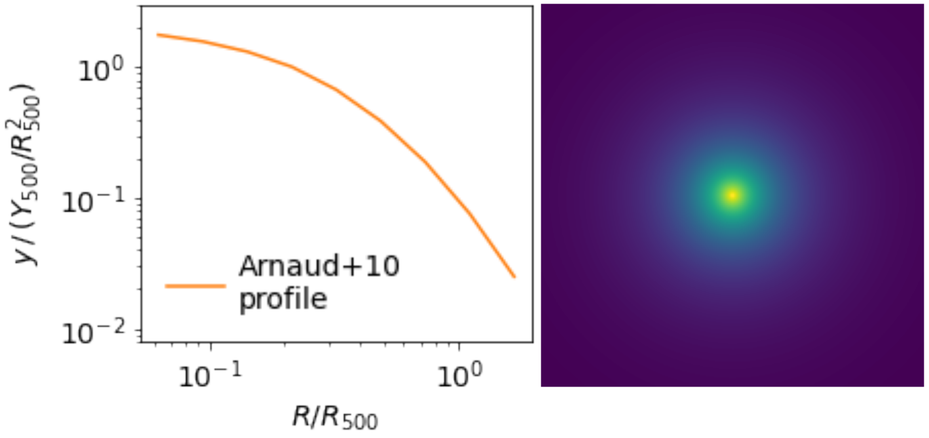

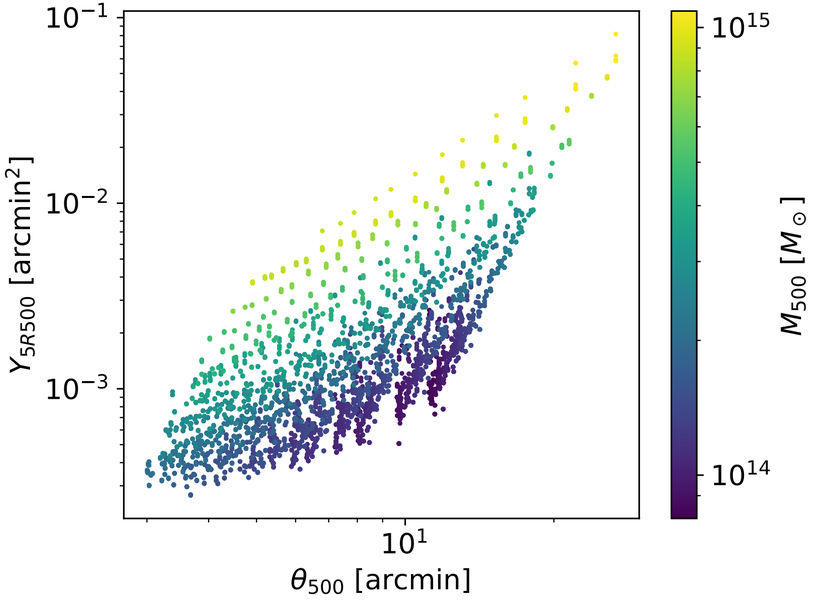

Results

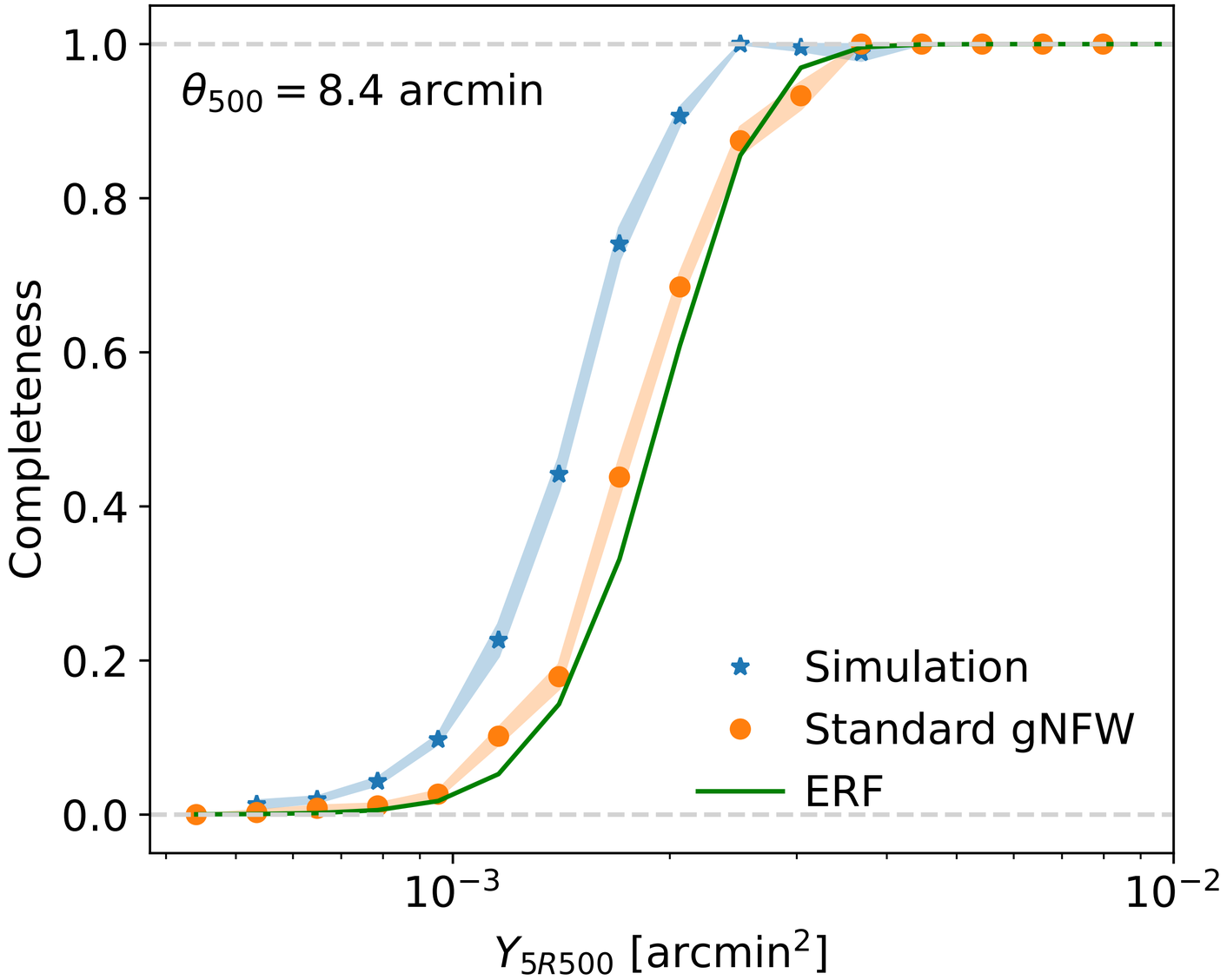

Completeness of spherical images ~ analytical ERF estimation

BUT

Simulation images show higher completeness than spherical ones

Results

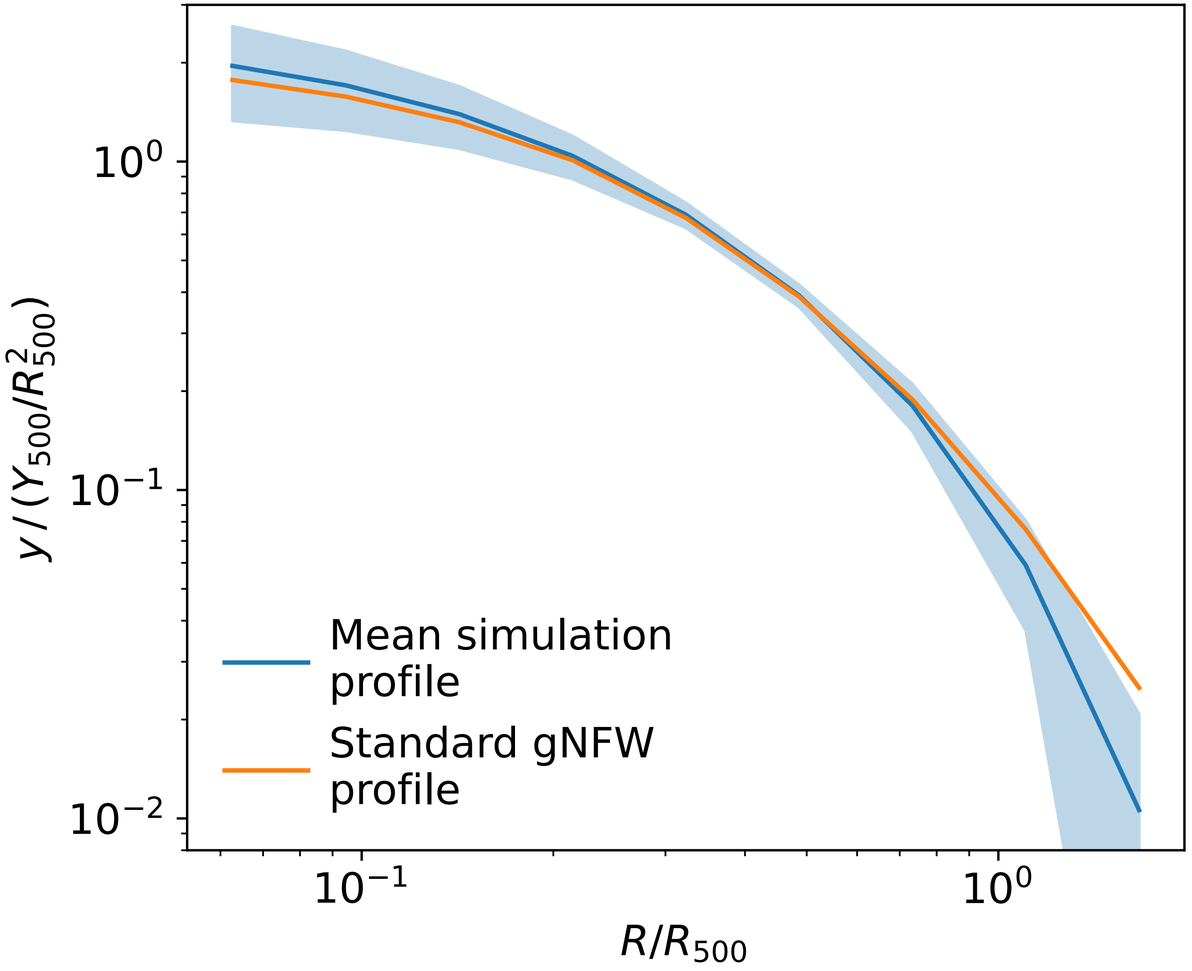
10^0
10^{-1}
10^{-2}
$y\,/\,(Y_{500}/R^2_{500})$
Mean simulation profile
Standard gNFW profile
10^{-1}
10^0
R/R_{500}

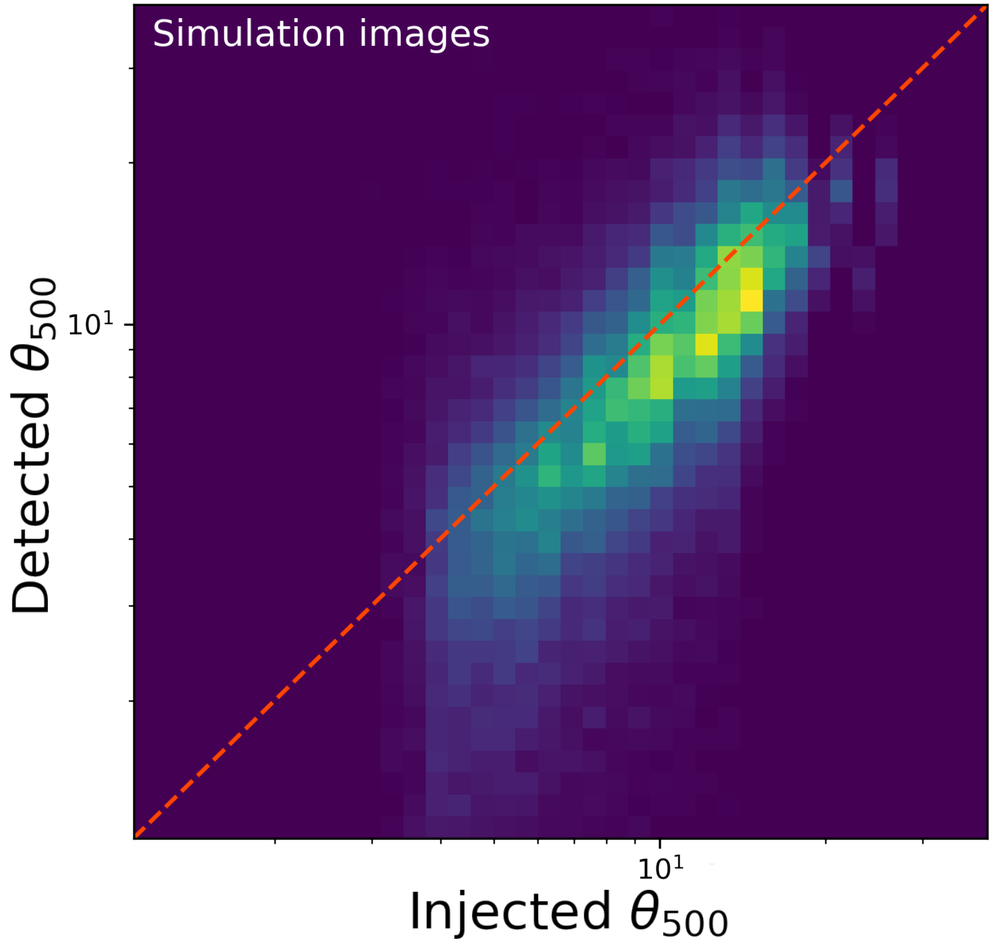
Simulation images
Detected θ_{500}
10^1
10^1
Injected θ_{500}

Results

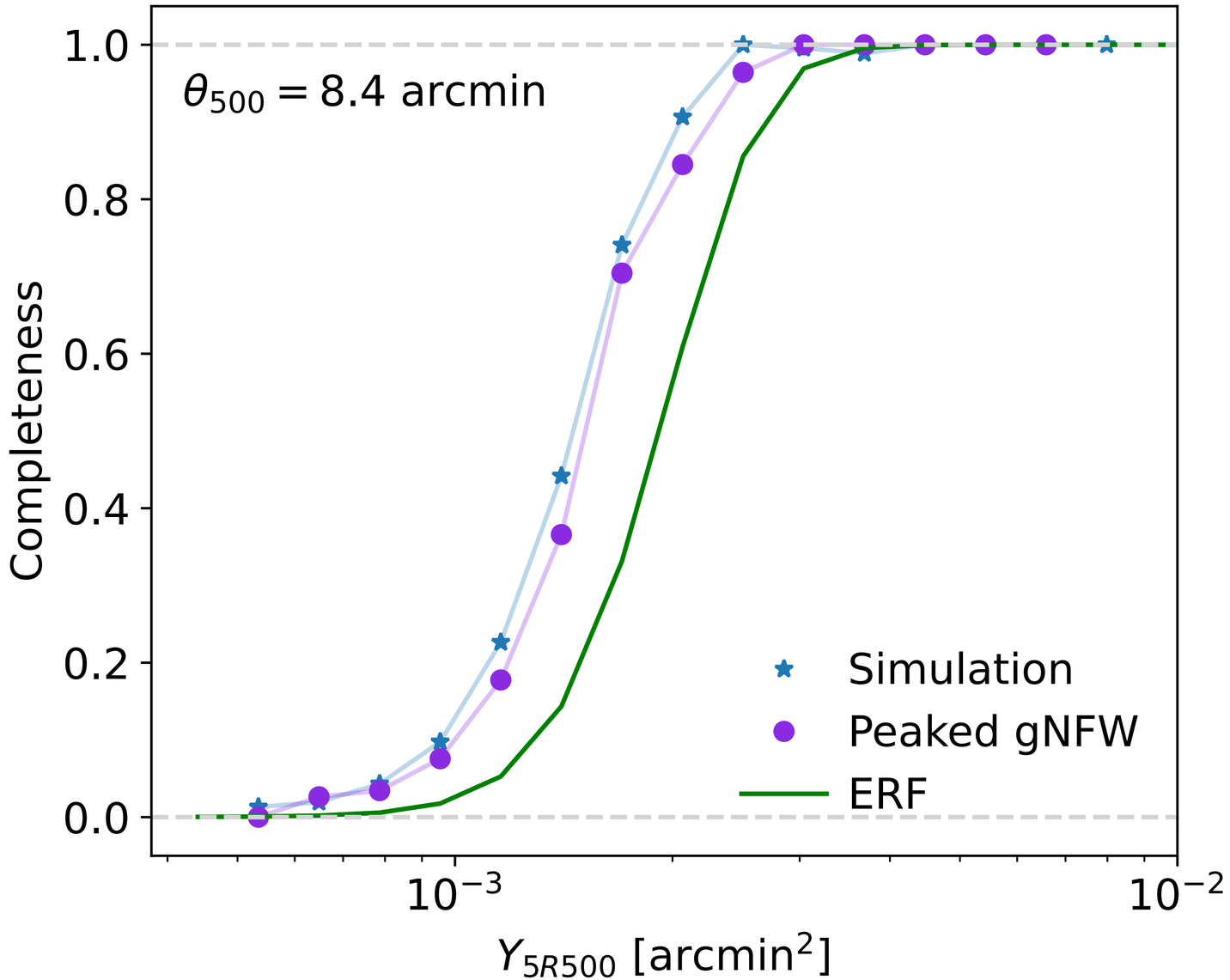

If we use a set of images with **higher concentration**, we get a completeness similar to the one of the **simulation images**

Results

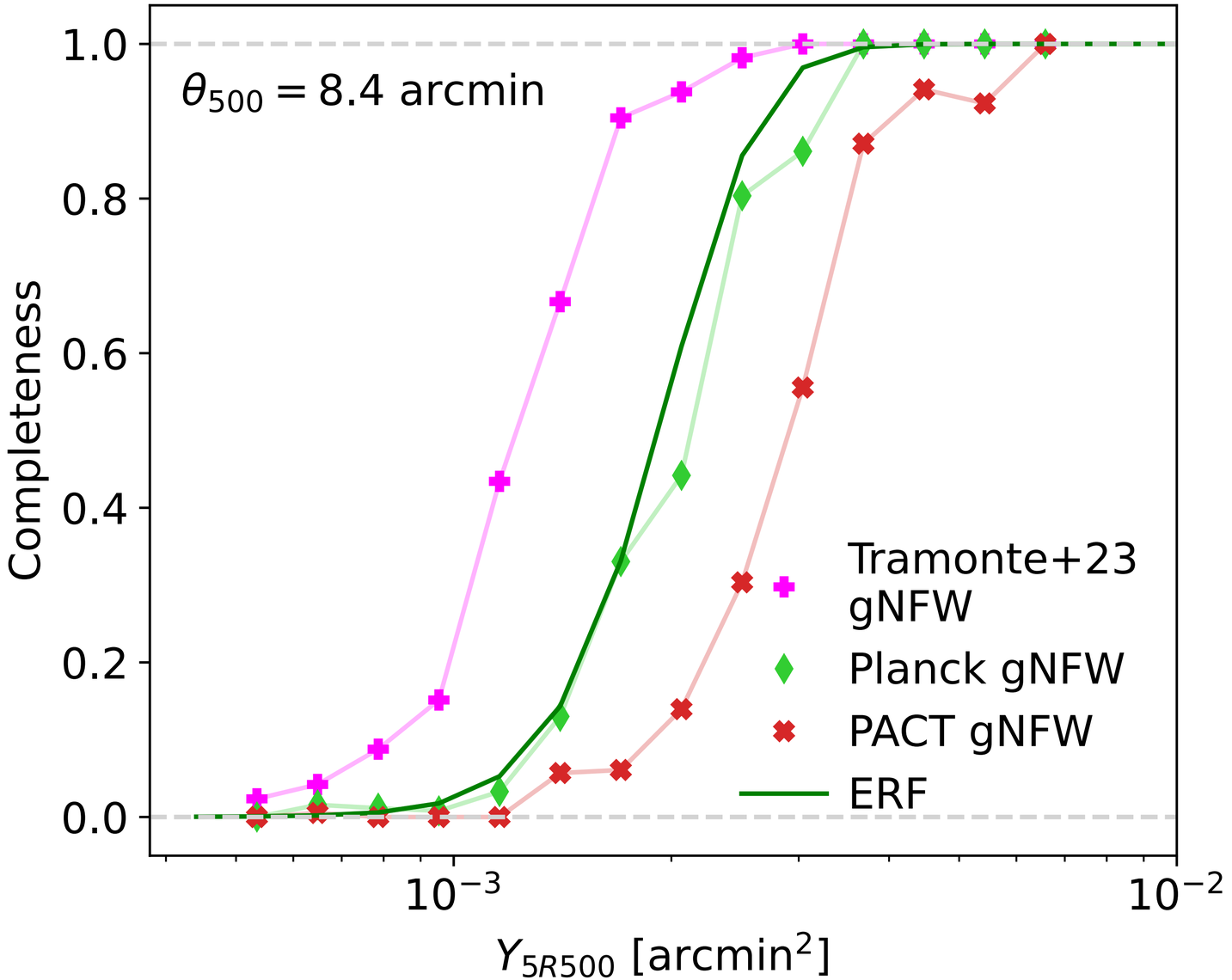

We test **different profiles** derived from observations, showing the spread it produces in the completeness

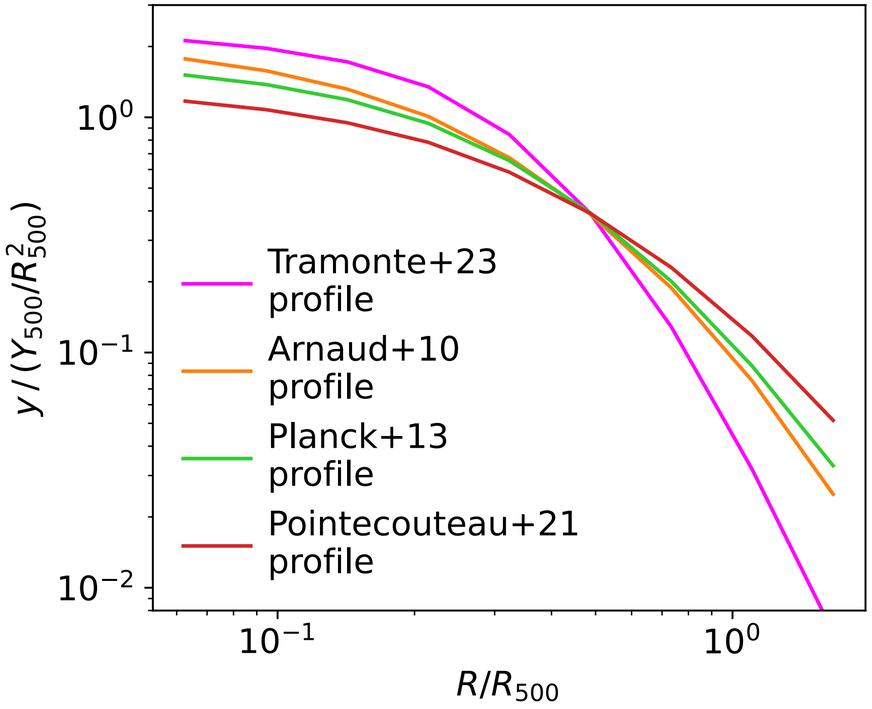

Results

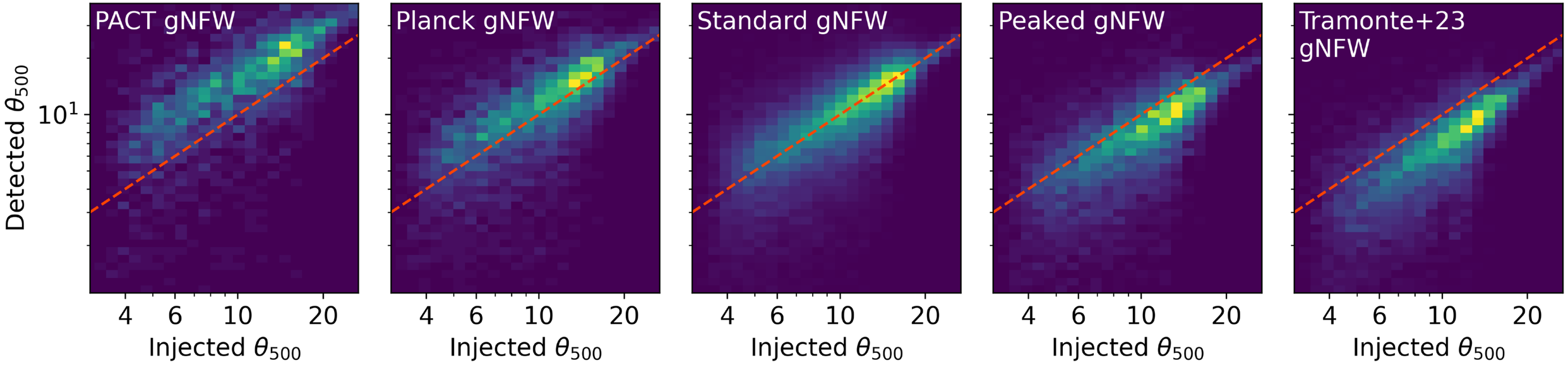

This test confirms the relation between the **steepness** of the pressure profile and the **bias** in the **detected cluster radii**

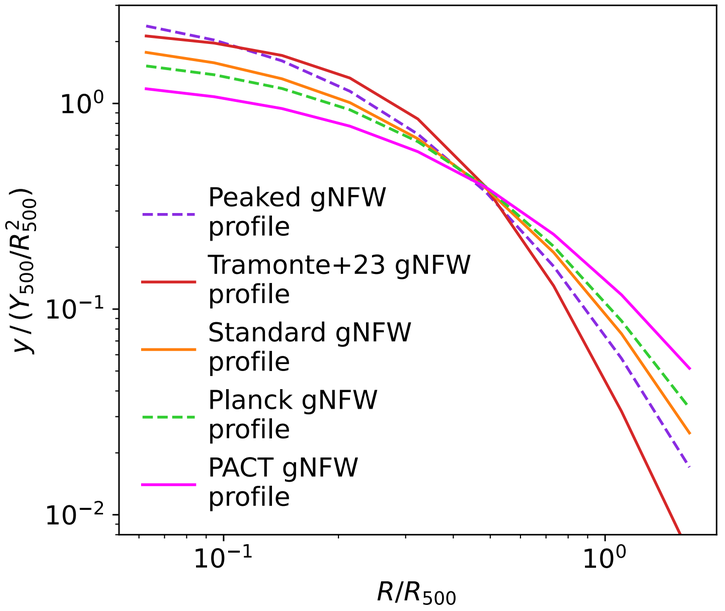

Impact on Cosmological Analysis

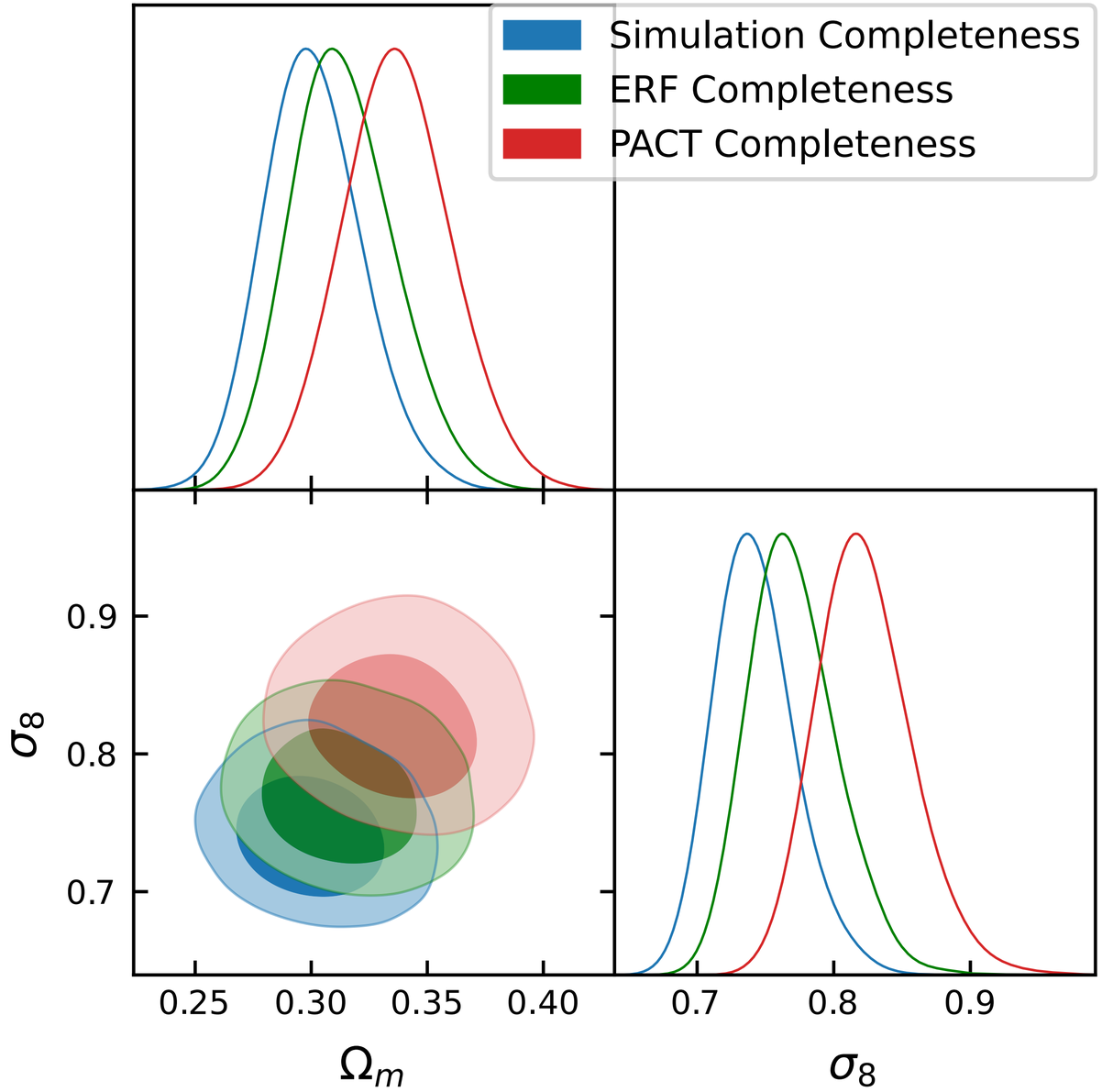

Testing the impact of two completeness cases on cosmological constraints

↓

Shift in (Ω_m, σ_8) space:

Higher completeness → **Lower values**

Lower completeness → **Higher values**

Impact on Cosmological Analysis

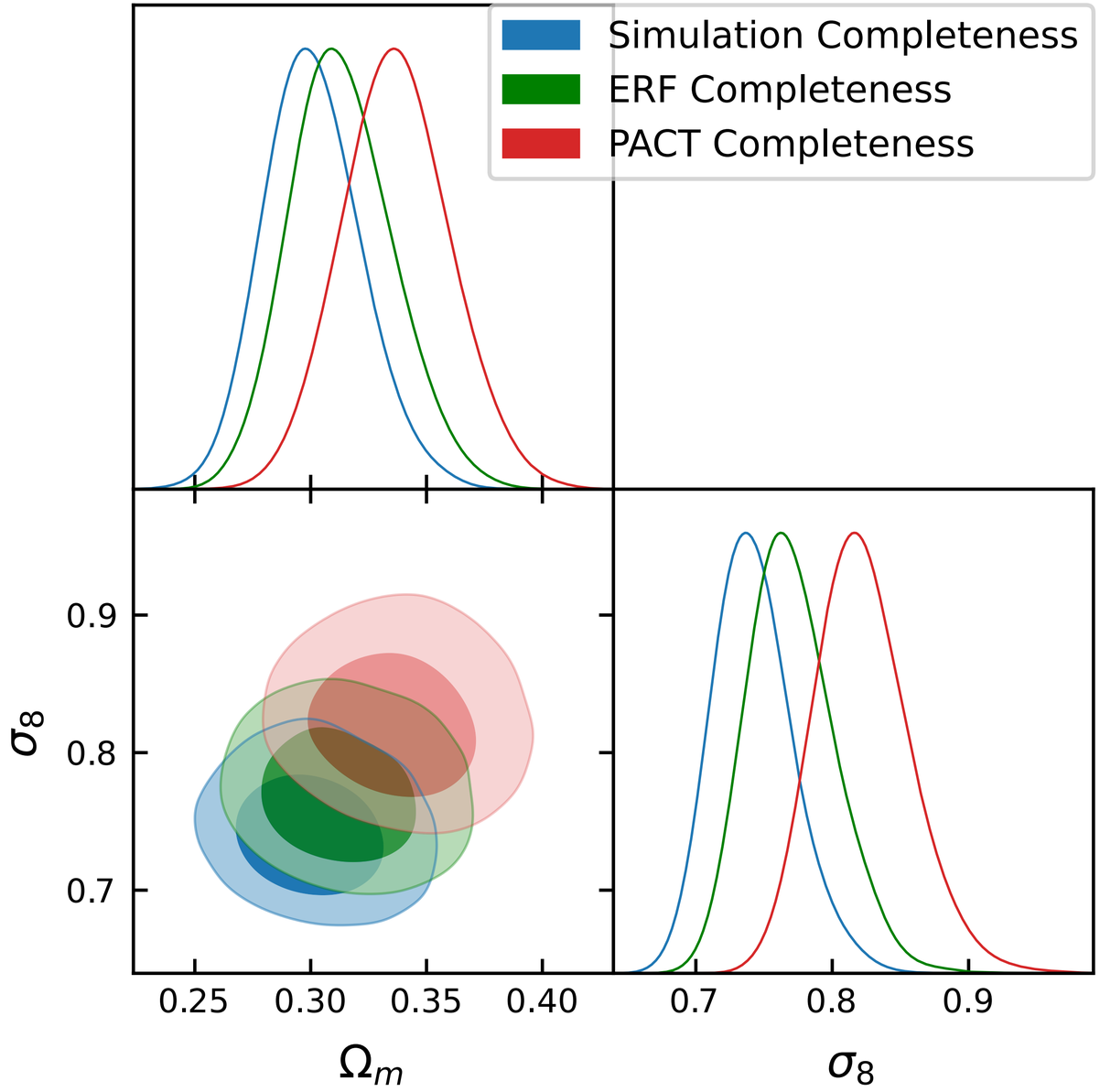

Shift in (Ω_m, σ_8) space similar to changing the scaling relations priors

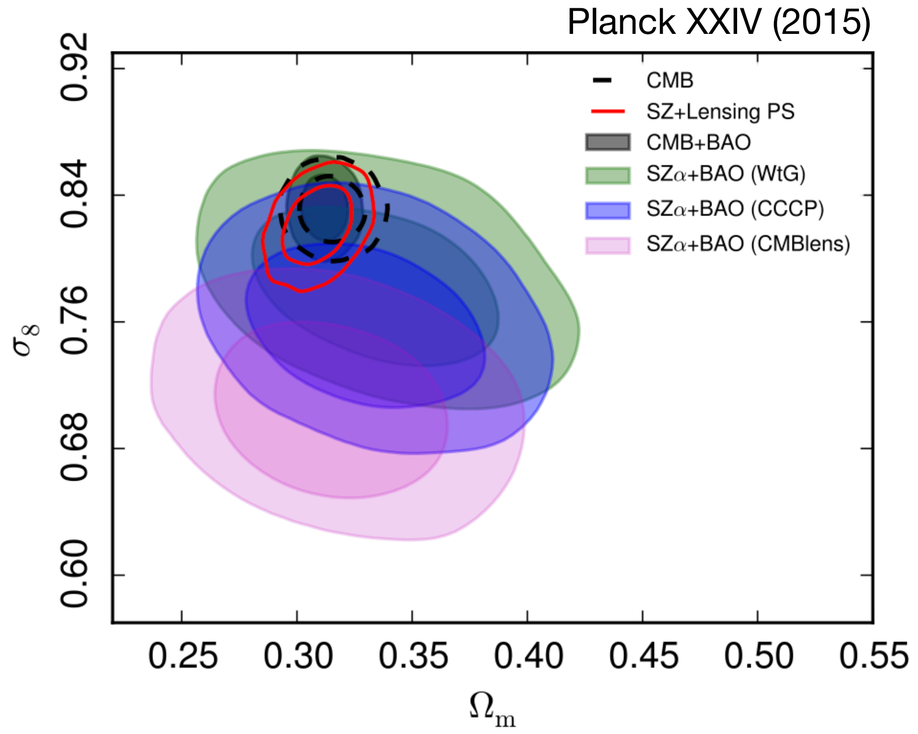

Conclusions

- These results suggest that the completeness depends on **different cluster parameters** beyond those of the ERF estimate.

- In particular, we see how a **steeper** cluster profile leads to an increased probability of detection, while a **flatter** profile reduces it.

- Furthermore, we tested the impact of **cluster morphology** on the completeness, finding that more elliptical objects are slightly more difficult to detect.

- Changing the completeness in the cosmological analysis moves the constraints on (Ω_m, σ_8) along the same direction of the mass scaling relations.

→ Need for more precise determination of clusters' profiles

Thank you

Backup

Cluster images

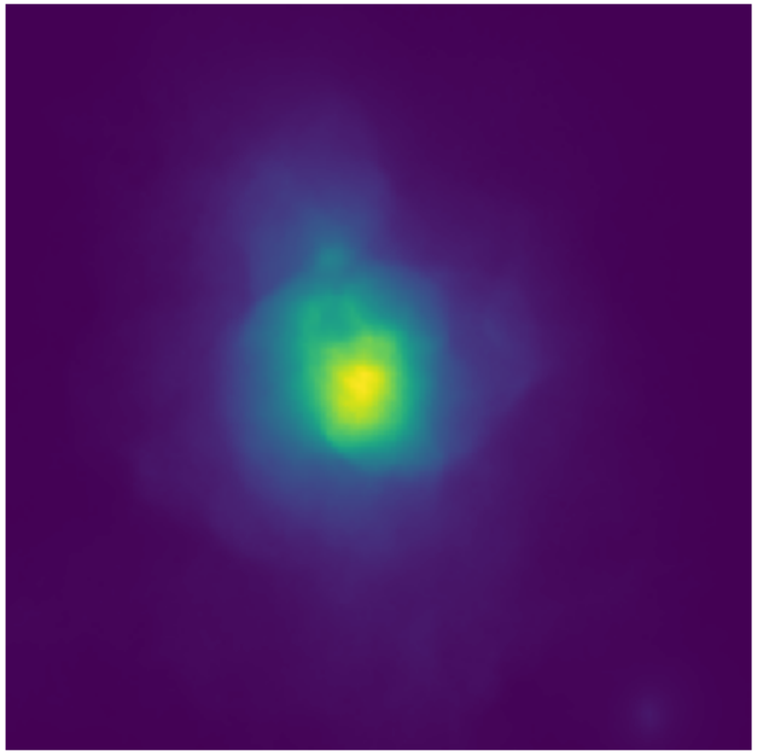

Simulation

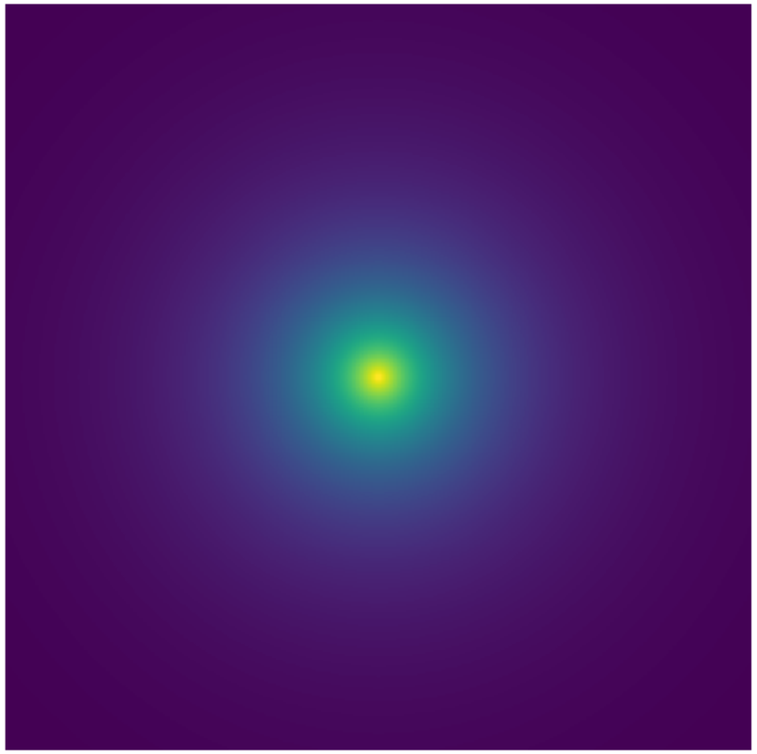

gNFW

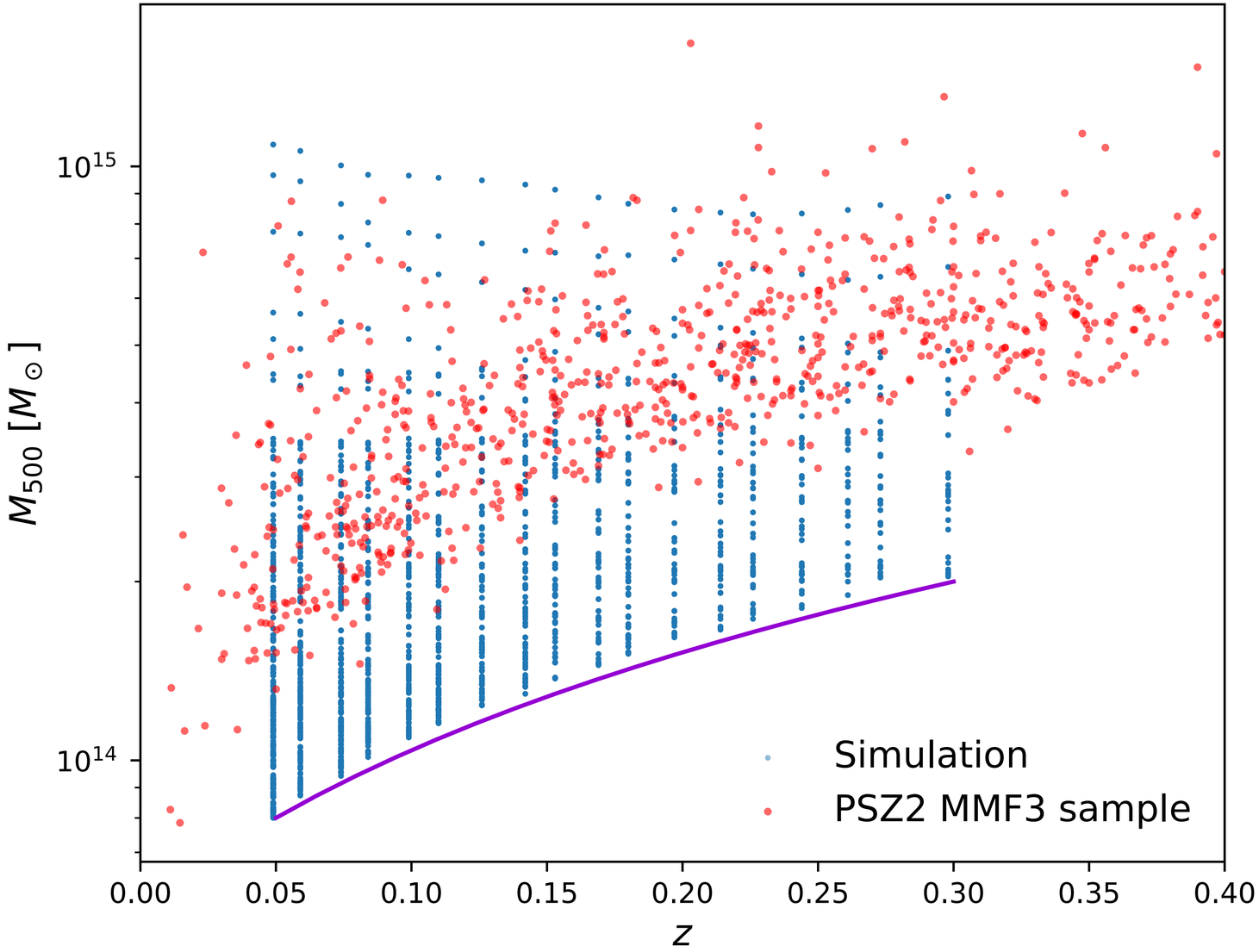
10^{15}
10^{14}
M_{500} [$M_\odot$]
0.00
0.05
0.10
0.15
0.20
0.25
0.30
0.35
0.40
z
Simulation
PSZ2 MMF3 sample

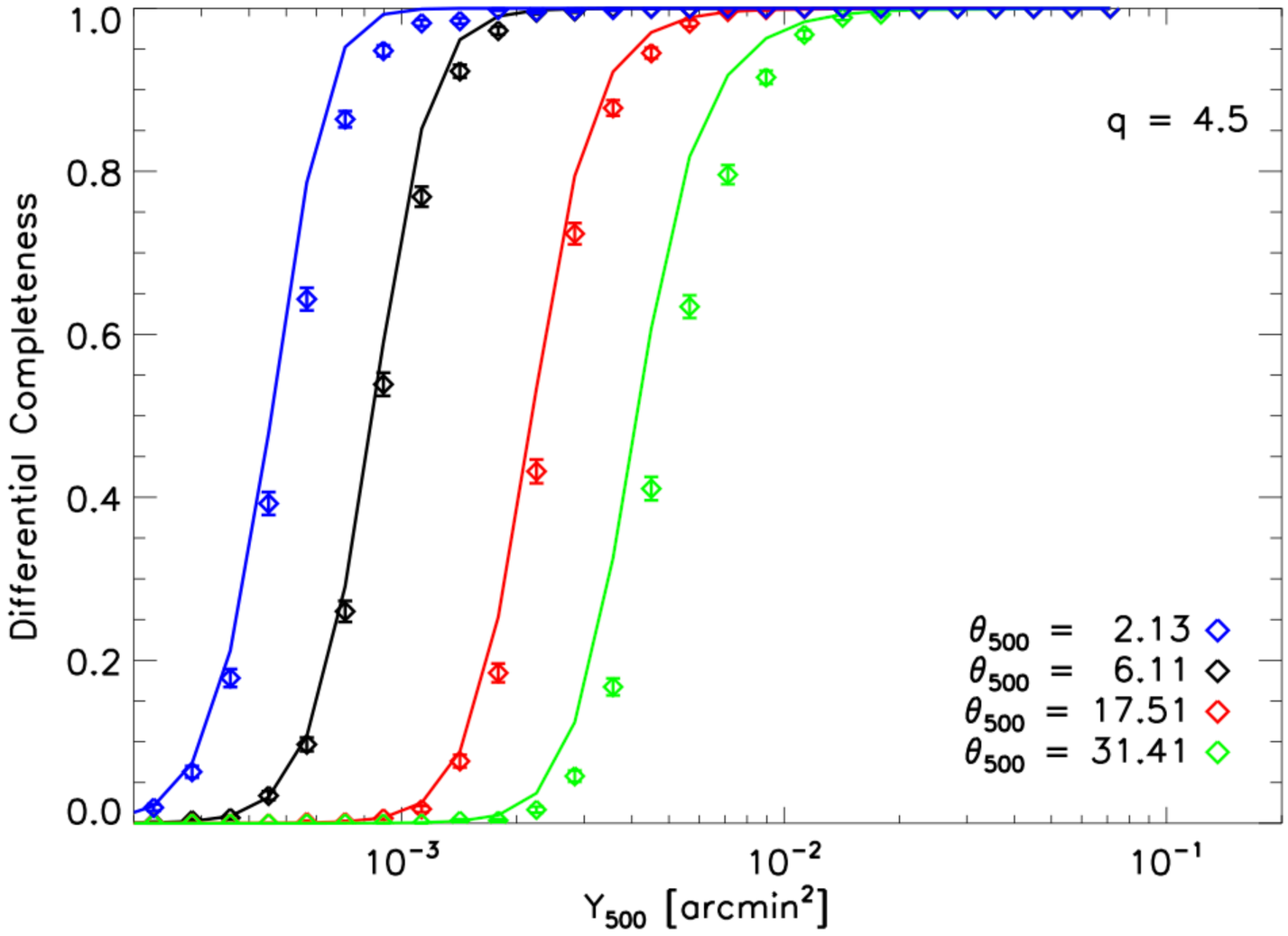

Planck XXVII 2015

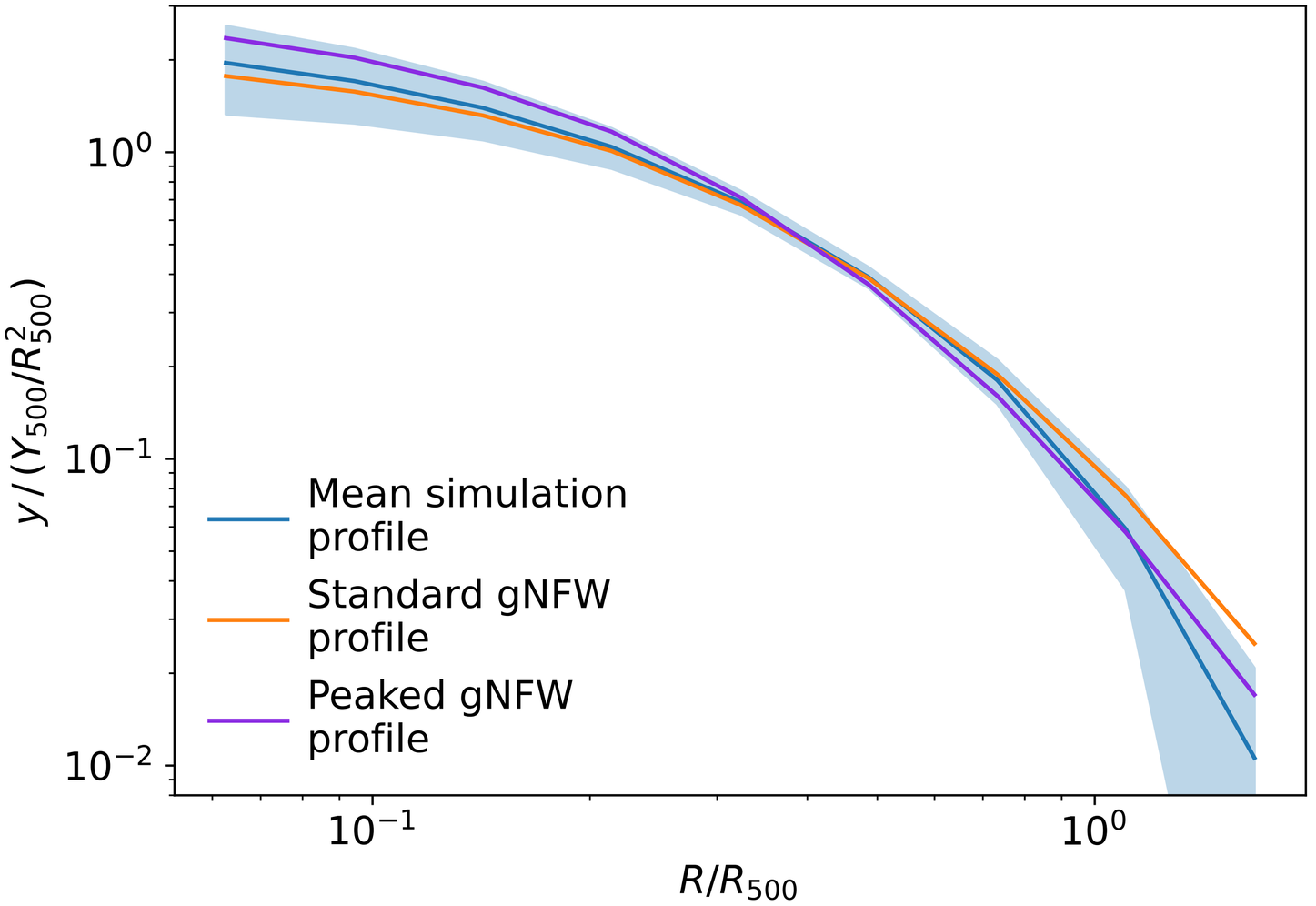
10^0
10^{-1}
10^{-2}
$y\,/\,(Y_{500}/R^2_{500})$
10^{-1}
10^0
R/R_{500}
Mean simulation profile
Standard gNFW profile
Peaked gNFW profile

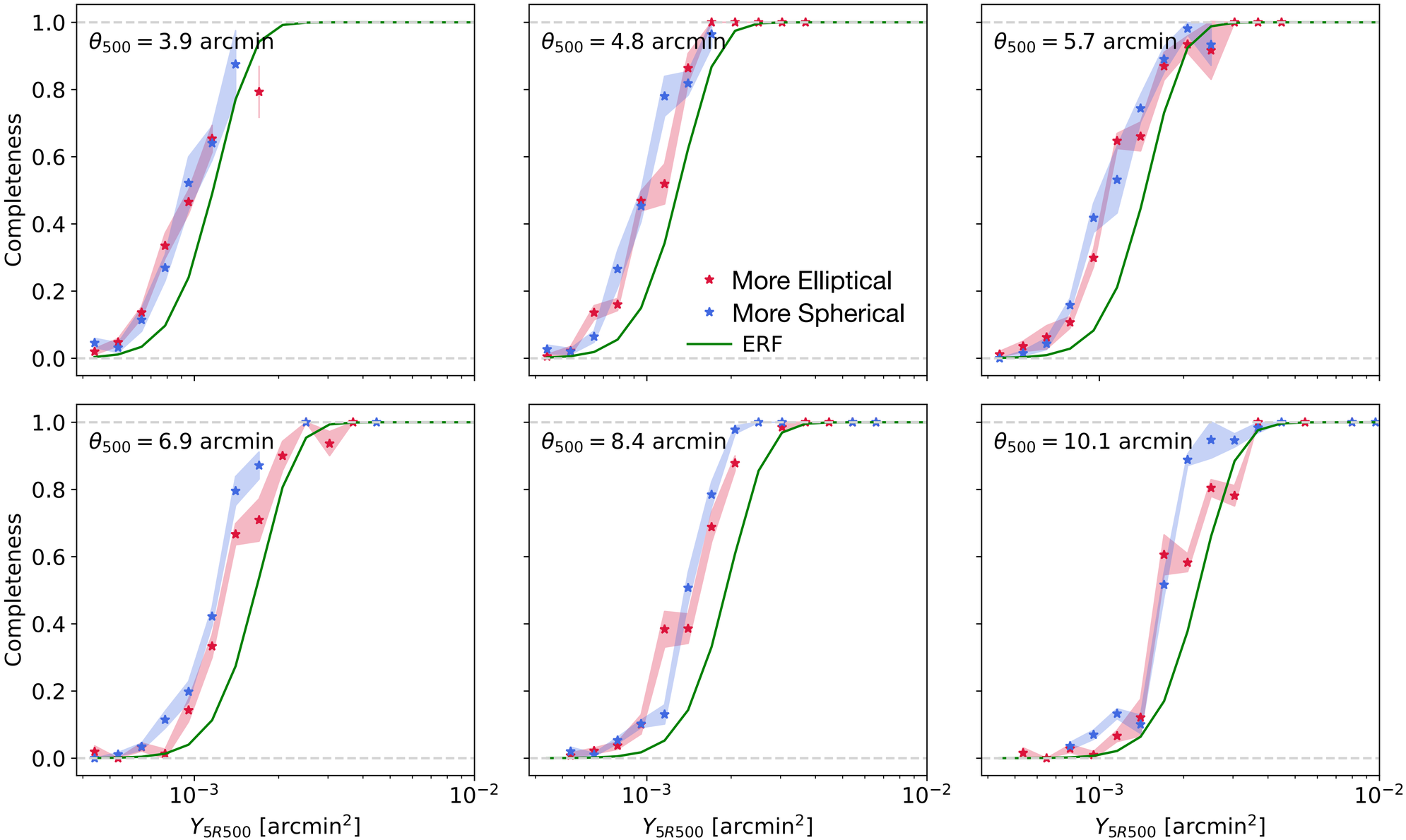
$\theta_{500} = 3.9$ arcmin
$\theta_{500} = 4.8$ arcmin
$\theta_{500} = 5.7$ arcmin
$\theta_{500} = 6.9$ arcmin
$\theta_{500} = 8.4$ arcmin
$\theta_{500} = 10.1$ arcmin
More Elliptical
More Spherical
ERF
Completeness
Y_{5R500} [arcmin^2]
1.0
0.8
0.6
0.4
0.2
0.0
10^{-3}
10^{-2}

Impact on Cosmological Analysis

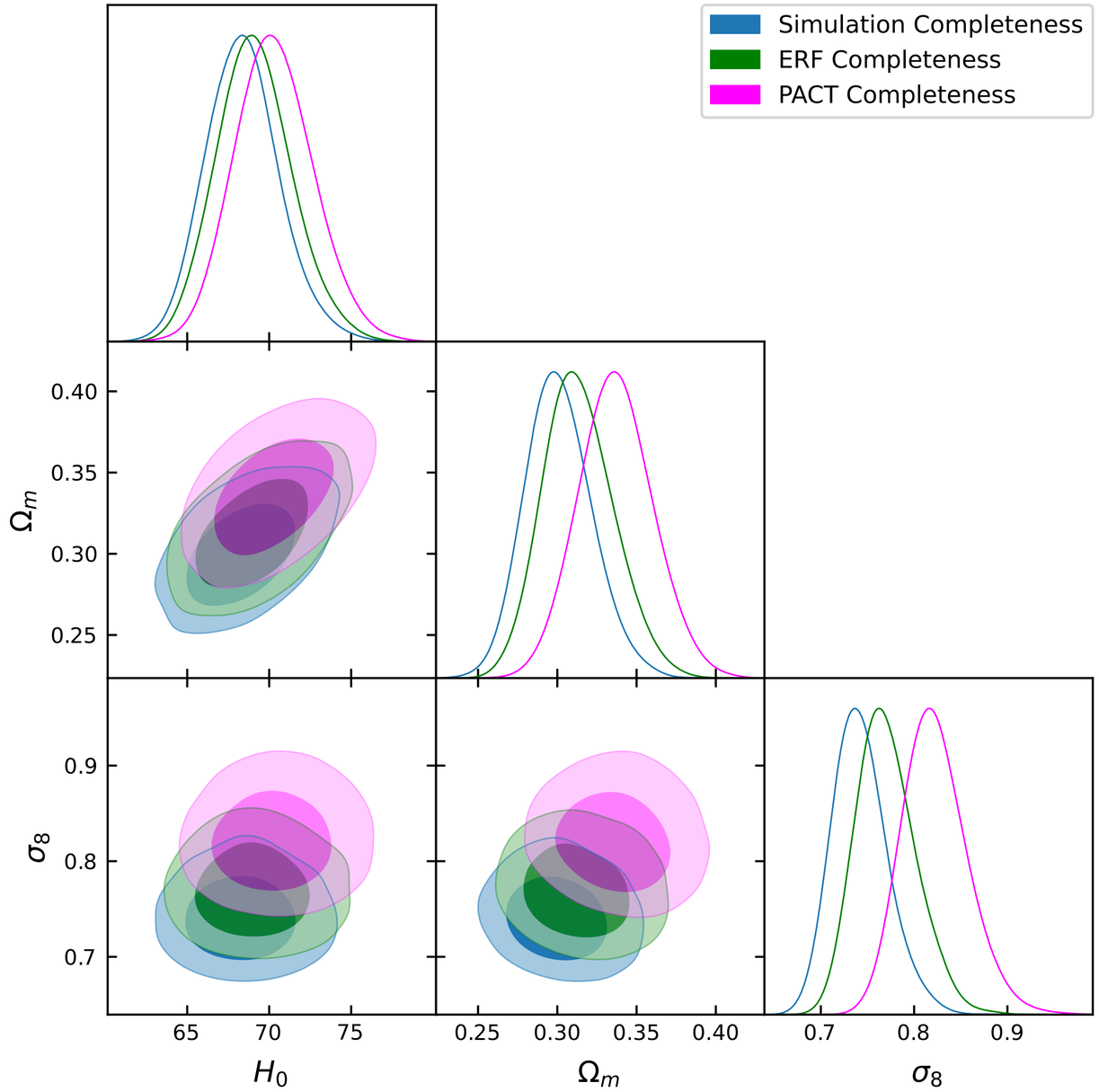

Impact on Cosmological Analysis